A Contrast Source Inversion Scheme for Imaging Acoustic Contrast

Koen W.A. van Dongen[†] and William M.D. Wright[*]

Ultrasonics Research Group
Department of Electrical and Electronic Engineering
University College Cork, Cork
IRELAND

E-mail: [†]koen@rennes.ucc.ie [*]bill.wright@ucc.ie

Abstract — **In this paper we present an inversion method which allows the reconstruction of density and compressibility profiles from measured scattered acoustic pressure and velocity data. The imaging method is based on a complete three-dimensional vectorial description of the acoustic wave fields. A conjugate gradient scheme is used to solve the corresponding integral equations iteratively. In order to regularize the inverse problem, a contrast source formulation is used. Good results are obtained with this novel imaging method when tested on synthetic data.**

I Introduction

Acoustic wave fields are used in a wide range of applications to probe the interior of objects in a nondestructive and noninvasive manner. The scale on which this takes place varies from the kilometer range in the oil and gas industry down to the millimeter range in medical applications. One of the medical applications we are interested in is hyperthermia cancer treatment. In this case, acoustic wave fields are used to measure during or directly after the treatment the acoustic medium parameters in and around the tumor in order to investigate the effect of the treatment. Next, changes in the medium parameters of the tissue are related to changes in temperature[1]. Consequently, there is a demand for imaging methods which reconstruct these velocity profiles with high accuracy.

In this paper we investigate a novel method to localize and characterize three dimensional objects from measured scattered acoustic pressure and velocity wave fields. Contrast functions are used to describe the variations present in the acoustic medium parameters; the volume density of mass and the compressibility. The scattering mechanism is formulated via two integral equations of the second type, one for the pressure and one for the velocity wave field.

During the forward problem, the integral equations are solved for known incident wave fields, known contrast functions and unknown scattered wave fields. The inverse problem refers to the situation where a solution is obtained for the unknown contrast function for known incident and measured scattered wave fields[2]. It is well known that this inverse problem is ill-posed. Therefore, many imaging methods rely on reducing the number of unknowns by describing the scattering mechanism as a function of a single contrast function, e.g. changes in speed of sound only. In this case, a scalar formulation of the problem is sufficient.

In this paper, we discuss a novel technique based on a vectorial description of the wave field problem. This method allows the reconstruction of both the density and the compressibility from measured acoustic data by using minimization method based on a conjugate gradient inversion scheme. In a standard conjugate gradient inversion scheme the L_2-norm of a single error function is minimized iteratively. This error function is defined as the residual of the measured scattered wave field minus the computed scattered wave field based on the approximate solution. In order to regularize the problem, a contrast source formulation is used which splits the error functional into two parts.

Note that, similar problems play an important role in electromagnetic scattering problems. Here, contrasts are defined via changes in the complex permittivity and/or magnetic permeability. In this area, good results are recently obtained by Van den Berg and Abubakar[3] by using a contrast source formulations similar to the one formulated in this paper.

II Forward Problem

The formulation of the scattering problem is done in the temporal Laplace domain with Laplace pa-

rameter $\hat{s}$. Results for the frequency domain Ω are obtained by taking the limit $\hat{s} \rightarrow -i\omega$, with $i^2 = -1$ and ω the temporal angular frequency. The symbol "$\hat{}$" on top of a parameter is used to show its temporal dependency. Positions in the spatial domain $\mathbb{R}^3$ are notated as a vector x_m or x_n, with $\{m, n\} = 1, 2$ or 3.

Combining reciprocity[4] with the acoustic wave field equations results in an expression for the total pressure wave field $\hat{p}^{\text{tot}}(x_m)$ and the total velocity wave field $\hat{v}_i^{\text{tot}}(x_m)$ for $\{i, j\} = 1, 2$ or 3 which reads

$$\hat{p}^{\text{tot}}(x_m) = \hat{p}^{\text{inc}}(x_m) + \hat{p}^{\text{sct}}(x_m)\,, \tag{1}$$
$$\hat{v}_i^{\text{tot}}(x_m) = \hat{v}_i^{\text{inc}}(x_m) + \hat{v}_i^{\text{sct}}(x_m)\,, \tag{2}$$

where $\hat{p}^{\text{inc}}(x_m)$ and $\hat{v}_k^{\text{inc}}(x_m)$ are the incident pressure and velocity fields and where $\hat{p}^{\text{sct}}(x_m)$ and $\hat{v}_i^{\text{sct}}(x_m)$ refer to the scattered pressure and velocity fields. In the presence of acoustic contrasts in the homogenous background medium these scattered wave fields equal

$$\begin{aligned}\hat{p}^{\text{sct}}(x_m) &= \hat{\mathcal{G}}^{pq}(x_m, x_n)\Delta\hat{\eta}(x_n)\hat{p}^{\text{tot}}(x_n) \\ &\quad + \hat{\mathcal{G}}_i^{pf}(x_m, x_n)\Delta\hat{\zeta}(x_n)\hat{v}_i^{\text{tot}}(x_n)\,, \end{aligned}\tag{3}$$
$$\begin{aligned}\hat{v}_i^{\text{sct}}(x_m) &= \hat{\mathcal{G}}_i^{vq}(x_m, x_n)\Delta\hat{\eta}(x_n)\hat{p}^{\text{tot}}(x_n) \\ &\quad + \hat{\mathcal{G}}_{i,j}^{vf}(x_m, x_n)\Delta\hat{\zeta}(x_n)\hat{v}_j^{\text{tot}}(x_n)\,, \end{aligned}\tag{4}$$

where the contrasts functions $\Delta\hat{\eta}(x_n)$ and $\Delta\hat{\zeta}(x_n)$ are defined by variations in the acoustic medium parameters compressibility κ and density ρ of the background medium (bg) and the object medium (obj) via

$$\Delta\hat{\eta}(x_n) = \hat{s}\Delta\kappa(x_n) = \hat{s}\left(\kappa^{\text{bg}} - \kappa^{\text{obj}}(x_n)\right)\,, \tag{5}$$
$$\Delta\hat{\zeta}(x_n) = \hat{s}\Delta\rho(x_n) = \hat{s}\left(\rho^{\text{bg}} - \rho^{\text{obj}}(x_n)\right)\,. \tag{6}$$

The Green's tensor functions shown in equations (3) and (4) are defined as follows

$$\hat{\mathcal{G}}^{pq}(x_m, x_n)\hat{q}(x_n) = \zeta^{\text{bg}}\hat{G}(x_m, x_n) * \hat{q}(x_n)\,, \tag{7}$$
$$\hat{\mathcal{G}}_i^{pf}(x_m, x_n)\hat{f}_i(x_n) = -\partial_i\Big[\hat{G}(x_m, x_n) * \hat{f}_i(x_n)\Big], \tag{8}$$
$$\hat{\mathcal{G}}_i^{vq}(x_m, x_n)\hat{q}(x_n) = -\partial_i\Big[\hat{G}(x_m, x_n) * \hat{q}(x_n)\Big], \tag{9}$$
$$\begin{aligned}\hat{\mathcal{G}}_{i,j}^{vf}(x_m, x_n)\hat{f}_j(x_n) = \frac{1}{\zeta^{\text{bg}}}\{ &\\ \partial_i\partial_j\left[\hat{G}(x_m, x_n) * \hat{f}_j(x_n)\right] &\\ +\delta_{i,j}\delta(x_m - x_n) * \hat{f}_j(x_n)\Big\}, &\end{aligned}\tag{10}$$

with ∂_i the spatial derivative in the x_i direction, $\delta_{i,j}$ Kronecker's delta function, $\delta(x_m - x_n)$ the impulse response function, $\hat{G}(x_m, x_n)$ the scalar form of Green's function, $\hat{q}(x_n)$ a volume density of injection rate source and $\hat{f}_j(x_n)$ a volume density of force. Note that, $f(x_m, x_n) * g(x_n)$ refers to a convolution of the functions $f(x_n)$ and $g(x_n)$ over the spatial domain $\mathbb{D}$. A solution for the forward problem is obtained by using a standard conjugate gradient inversion scheme, as described by Kleinman and Van den Berg[5].

III Inverse Problem

The aim is to compute the contrast functions of the acoustic medium parameters compressibility κ and density ρ by solving the set of integral equations stated in equations (1)-(10) for known measured scattered acoustic wave fields. Due to the ill-posed nature of the inverse problem they can not be solved with a standard conjugate gradient inversion scheme and regularization is required. This regularization is obtained by using a contrast source formulation.

a) Contrast Source Formulation

Examining equations (3) and (4) reveals that the sources generating the scattered wave fields are defined as the product of two contrast functions with corresponding total wave fields. Combining these terms lead to an expression for the contrast sources, $\hat{w}_k^p(x_m)$ and $\hat{w}_{i,k}^v(x_m)$, which read

$$\hat{w}_k^p(x_m) = \hat{s}\Delta\kappa(x_m)\hat{p}_k^{\text{tot}}(x_m)\,, \tag{11}$$
$$\hat{w}_{i,k}^v(x_m) = \hat{s}\Delta\rho(x_m)\hat{v}_{i,k}^{\text{tot}}(x_m)\,, \tag{12}$$

where the subscript $k = 1, \ldots, K$ refers to the spatial position of the transmitter which generates the incident wave field. Consequently, equations (3) and (4) can be formulated as

$$\begin{aligned}\hat{p}_k^{\text{sct}}(x_m) &= \hat{\mathcal{G}}^{pq}(x_m, x_n)\hat{w}_k^p(x_n) \\ &\quad + \hat{\mathcal{G}}_i^{pf}(x_m, x_n)\hat{w}_{i,k}^v(x_n)\,, \end{aligned}\tag{13}$$
$$\begin{aligned}\hat{v}_{i,k}^{\text{sct}}(x_m) &= \hat{\mathcal{G}}_i^{vq}(x_m, x_n)\hat{w}_k^p(x_n) \\ &\quad + \hat{\mathcal{G}}_{i,j}^{vf}(x_m, x_n)\hat{w}_{j,k}^v(x_n)\,. \end{aligned}\tag{14}$$

Combining equations (11)-(14) leads to a reformulation of the contrast sources as follows

$$\begin{aligned}\hat{w}_k^p(x_m) &= \hat{s}\Delta\kappa(x_m)\hat{p}_k^{\text{inc}}(x_m) \\ &\quad + \hat{s}\Delta\kappa(x_m)\hat{\mathcal{G}}^{pq}(x_m, x_n)\hat{w}_k^p(x_n) \\ &\quad + \hat{s}\Delta\kappa(x_m)\hat{\mathcal{G}}_i^{pf}(x_m, x_n)\hat{w}_{i,k}^v(x_n)\,, \end{aligned}\tag{15}$$
$$\begin{aligned}\hat{w}_{i,k}^v(x_m) &= \hat{s}\Delta\rho(x_m)\hat{v}_{i,k}^{\text{inc}}(x_m) \\ &\quad + \hat{s}\Delta\rho(x_m)\hat{\mathcal{G}}_i^{vq}(x_m, x_n)\hat{w}_k^p(x_n) \\ &\quad + \hat{s}\Delta\rho(x_m)\hat{\mathcal{G}}_{i,j}^{vf}(x_m, x_n)\hat{w}_{j,k}^v(x_n)\,. \end{aligned}\tag{16}$$

Based on the formulations used for equations (11)-(16), two sets of error functionals are defined. The first one is referred to as the error in the data equation and is based on the residual of the measured scattered wave fields minus the scattered wave fields based on the approximated

contrast sources. Hence, at the N^{th} iteration step this error functional reads

$$\begin{aligned}\hat{r}^p_{\mathbb{S};N;k}(x_m) &= \hat{p}^{\mathrm{sct}}_k(x_m) - \hat{\mathcal{G}}^{pq}_{\mathbb{S}}(x_m,x_n)\hat{w}^p_{N;k}(x_n) \\ &\quad - \hat{\mathcal{G}}^{pf}_i(x_m,x_n)\hat{w}^v_{N;i,k}(x_n)\,, \qquad (17)\\ \hat{r}^v_{\mathbb{S};N;i,k}(x_m) &= \hat{v}^{\mathrm{sct}}_{i,k}(x_m) - \hat{\mathcal{G}}^{vq}_i(x_m,x_n)\hat{w}^p_{N;k}(x_n) \\ &\quad - \hat{\mathcal{G}}^{vf}_{i,j}(x_m,x_n)w^v_{N;j,k}(x_n)\,, \qquad (18)\end{aligned}$$

with $\mathbb{S}$ the spatial domain containing the transducers. The second one is referred to as the error in the object equation and is based on the error in the computed contrast sources. Hence, this error functional equals

$$\begin{aligned}\hat{r}^p_{\mathbb{D};N;k}(x_m) &= \hat{s}\Delta\kappa_N(x_m)\hat{p}^{\mathrm{inc}}_k(x_m) - \hat{w}^p_{N;k}(x_m) \\ &\quad + \hat{s}\Delta\kappa(x_m)G^{pq}w^p_k(x_m) \\ &\quad + \hat{s}\Delta\kappa_N(x_m)\hat{\mathcal{G}}^{pf}_i\hat{w}^v_{N;i,k}(x_n)\,, \qquad (19)\\ \hat{r}^v_{\mathbb{D};N;i,k}(x_m) &= \hat{s}\Delta\rho_N(x_m)\hat{v}^{\mathrm{inc}}_{i,k}(x_m) - \hat{w}^v_{N;i,k}(x_m) \\ &\quad + \hat{s}\Delta\rho(x_m)G^{vq}_i w^p_k(x_m) \\ &\quad + \hat{s}\Delta\rho_N(x_m)\hat{\mathcal{G}}^{vf}_{i,j}\hat{w}^v_{N;j,k}(x_n)\,, \qquad (20)\end{aligned}$$

with $\mathbb{D}$ the spatial domain containing the contrast and hence the contrast sources. Next, we define the L_2-norm of the four-dimensional vector representing the acoustic wave fields in the spatial domain $\mathbb{S}$ as

$$\begin{aligned}\left\|\begin{pmatrix}\hat{p}_k(x_m)\\ \hat{v}_{i,k}(x_m)\end{pmatrix}\right\|^2_{\mathbb{S}} &= \sum_{x_m\in\mathbb{S},k,\Omega}\Bigg\{Z\hat{p}_k(x_m)\left[\hat{p}_k(x_m)\right]^* \\ &\quad + \sum_i \hat{v}_{i,k}(x_m)\left[\hat{v}_{i,k}(x_m)\right]^*\Bigg\}, \qquad (21)\end{aligned}$$

and the L_2-norm of a four-dimensional vector representing the contrast sources in the spatial domain $\mathbb{D}$ as

$$\begin{aligned}\left\|\begin{pmatrix}\hat{w}^p_k(x_m)\\ \hat{w}^v_{i,k}(x_m)\end{pmatrix}\right\|^2_{\mathbb{D}} &= \sum_{x_m\in\mathbb{D},k,\Omega}\Bigg\{\hat{w}^p_k(x_m)\left[\hat{w}^p_k(x_m)\right]^* \\ &\quad + \sum_i Z\hat{w}^v_{i,k}(x_m)\left[\hat{w}^v_{i,k}(x_m)\right]^*\Bigg\}, \qquad (22)\end{aligned}$$

where the constant Z is used to correct for differences in dimensions and is defined as

$$Z = \frac{\kappa^{\mathrm{bg}}}{\rho^{\mathrm{bg}}}\,. \qquad (23)$$

Finally, we define the normalized error functional

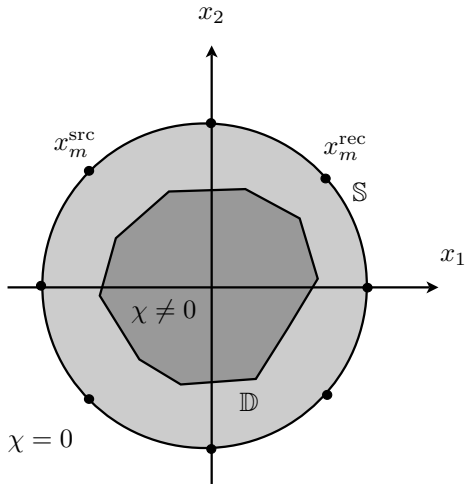

Fig. 1: The setup used for fan beam measurements

Err_N as

$$\begin{aligned}Err_N = &\frac{\left\|\begin{pmatrix}\hat{r}^p_{\mathbb{S};N;k}(x_m)\\ \hat{r}^v_{\mathbb{S};N;i,k}(x_m)\end{pmatrix}\right\|^2_{\mathbb{S}}}{\left\|\begin{pmatrix}\hat{p}^{\mathrm{sct}}_k(x_m)\\ \hat{v}^{\mathrm{sct}}_{i,k}(x_m)\end{pmatrix}\right\|^2_{\mathbb{S}}} \\ &+ \frac{\left\|\begin{pmatrix}\hat{r}^p_{\mathbb{D};N;k}(x_m)\\ \hat{r}^v_{\mathbb{D};N;i,k}(x_m)\end{pmatrix}\right\|^2_{\mathbb{D}}}{\left\|\begin{pmatrix}\Delta\hat{\eta}_{N-1}(x_m)\hat{p}^{\mathrm{inc}}_k(x_m)\\ \Delta\hat{\zeta}_{N-1}(x_m)\hat{v}^{\mathrm{inc}}_{i,k}(x_m)\end{pmatrix}\right\|^2_{\mathbb{D}}}\,, \qquad (24)\end{aligned}$$

with $\Delta\hat{\eta}_N(x_m)$ and $\Delta\hat{\zeta}_N(x_m)$ based on the approximated medium parameters of the objects. These medium parameters are obtained via direct minimization of the cost functionals in equations (19) and (20), consequently

$$\kappa^{\mathrm{obj}}_N(x_m) = \kappa^{\mathrm{bg}} - \frac{\sum_{k,\Omega}\Re\left[\hat{s}\hat{p}^{\mathrm{tot}}_{N;k}(x_m)\hat{w}^p_{N;k}(x_m)\right]}{\sum_{k,\Omega}\left|\hat{s}\hat{p}^{\mathrm{tot}}_{N;k}(x_m)\right|^2}\,, \qquad (25)$$

$$\rho^{\mathrm{obj}}_N(x_m) = \rho^{\mathrm{bg}} - \frac{\sum_{i,k,\Omega}\Re\left[\hat{s}\hat{v}^{\mathrm{tot}}_{N;i,k}(x_m)\hat{w}^v_{N;i,k}(x_m)\right]}{\sum_{i,k,\Omega}\left|\hat{s}\hat{v}^{\mathrm{tot}}_{N;i,k}(x_m)\right|^2}\,. \qquad (26)$$

Consequently, a conjugate gradient minimizations scheme is used to construct the contrast sources. After each update of the contrast sources, the contrast function is obtained via direct minimization.

IV Results and Discussion

The integral formulation shown in equations (1)-(10) is applied to the situation shown in Fig. 1.

Table 1: The medium parameters compressibility, κ, density, ρ, and speed of sound, c, for various tissues [6], [7], [8].

	κ $[10^{-9}\ (\text{Pa})^{-1}]$	ρ $[\text{kg/m}^3]$	c [m/s]
$T = 37\ ^\circ\text{C}$	0.36648	1056.6	1607
$T = 45\ ^\circ\text{C}$	0.10533	1053.3	1612
$T = 50\ ^\circ\text{C}$	0.36571	1051.0	1613

Here, 36 transducers ($K = 36$) are positioned on the spatial circular domain $\mathbb{S}$ which encloses the circular cylindrical domain D containing the objects. Data is obtained for the situation where one transducer acts as a transmitter while the remainder act as receivers. A complete data set is obtained by rotating the transducer system in equiangular steps over 360° around the object.

Synthetic data has been computed based on the synthetic contrast function shown in Fig. 2(a) and 2(b). The medium parameters, see Table 1, correspond to the situation where in human liver tissue at 37 °C one lesion is heated to 45 °C and two lesions are heated to 50 °C. The three dimensional volume contains $32 \times 32 \times 4$ elements of size $2.5 \times 2.5 \times 2.5\ \text{mm}^3$. Each temporal signal contains 16 points, equally spread over the frequency domain $\Omega = [5, 156]$ k Hz.

An additional data set $\underline{\hat{p}}_k^{\text{sct}}(x_m)$ and $\underline{\hat{v}}_{i,k}^{\text{sct}}(x_m)$ is computed by adding 10% white noise to the measured scattered wave fields, hence

$$\underline{\hat{p}}_k^{\text{sct}}(x_m) = \hat{p}_k^{\text{sct}}(x_m) + \underline{r}\ \max\left(\left|\hat{p}_k^{\text{sct}}(x_m)\right|\right)\ , \quad (27)$$

$$\underline{\hat{v}}_{i,k}^{\text{sct}}(x_m) = \hat{v}_{i,k}^{\text{sct}}(x_m) + \underline{r}\ \max\left(\left|\hat{v}_{i,k}^{\text{sct}}(x_m)\right|\right)\ , \quad (28)$$

with random rational number $\underline{r} \in [-0.1, 0.1]$, $\max\left(|\hat{p}_k^{\text{sct}}(x_m)|\right)$ the maximum value present in the set of all absolute values of $\hat{p}_k^{\text{sct}}(x_m)$ and $\max\left(\left|\hat{v}_{i,k}^{\text{sct}}(x_m)\right|\right)$ the maximum value present in the set of all absolute values of $\hat{v}_{i,k}^{\text{sct}}(x_m)$.

In Fig. 2(c)-2(f) the results obtained with the contrast source formulation are shown. A velocity profile based on the synthetic and reconstructed medium parameters is shown in Fig. 3. The minimization process was stopped after 100 iterations. At this stage, further decrease in the error functional can be neglected as can been observed from Fig. 4.

A personal computer containing 1 GB of RAM has been used to perform the computations in approximately half a day. In the computational scheme there are present a large number of loops which can be performed in parallelized way. This makes the application ideal to be performed on a computer cluster in order to reduce the computational time.

By comparing the reconstructed profiles (compressibility, density and velocity) with the synthetic profiles it can be shown that the maximum relative error is below 0.3%, even in presence of 10% white noise. Finding a numerical solution for the noise is difficult, since noise is not covered in the set of equations describing the scattering mechanism. Consequently, the error functional has a slower converging rate when compared with a noise free signal. In the reconstructed images, the presence of noise is reflected by the large amount of small fluctuations in the reconstructed background medium surrounding the objects. Preprocessing the signal with various filtering techniques could be a solution to this problem.

V Conclusion

A novel imaging method has been presented which allows the reconstruction of both density and compressibility profiles from measured scattered acoustic pressure and velocity data. The imaging method is based on a complete three-dimensional vectorial description of the acoustic wave fields. In order to regularize the inverse problem, a contrast source formulation is used. Good results are obtained with this novel imaging method when tested on synthetic data with and without 10% white noise. The results show that the maximum error is less than 0.3% in all the reconstructed images.

Acknowledgments

This work was financially supported via a Marie Curie Intra-European fellowship. We also gratefully acknowledge all the fruitful discussions we had with Conor Brennan and Konstantin M. Bograchev. Finally, we would like to thank the Boole Centre for Research in Informatics, University College Cork, Ireland, for the usage of their computer facility.

References

[1] N.T. Sanghvi, R.S. Foster, F.J. Fry, R. Bihrle, C. Hennige and L.V. Hennige, "Ultrasound intracavity system for imaging, therapy planning and treatment of focal disease", *Proceedings IEEE Ultrasonics Symposium 1992*, Vol. 2, 1249-1253, 1992.

[2] A. Abubakar and T.M. Habashy and P.M. van den Berg and D. Gisolf, "The diagonalized contrast source approach: an inversion method beyond the Born approximation", *Inverse Problems*, vol. 21, no. 2, pp. 685-702, 2005.

[3] P.M. van den Berg and A. Abubakar, "Contrast source inversion of 3D objects with electric and magnetic contrasts", *2004 URSI/EMTS Proceedings of the international*

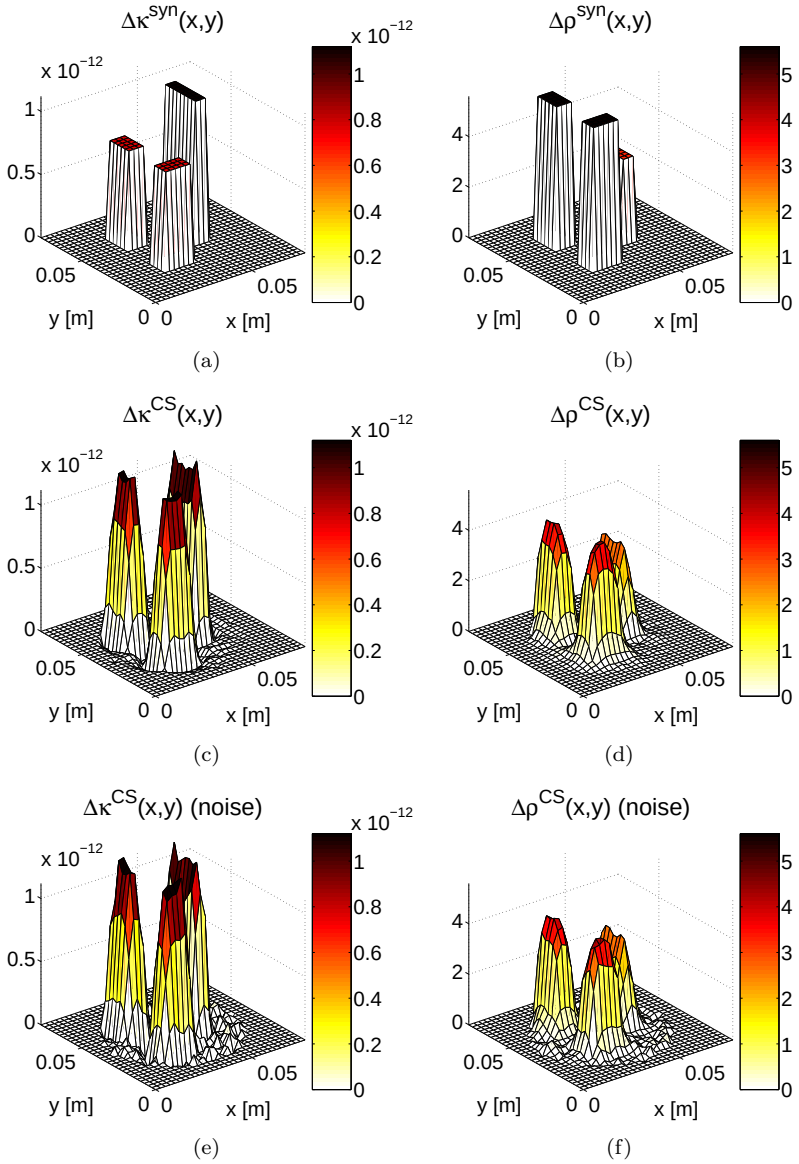

Fig. 2: A cross section of the synthetic and reconstructed contrast functions.

symposium on electromagnetic theory, pp. 700-702, 2004.

[4] A.T. de Hoop, *Handbook of radiation and scattering of waves: Acoustic Waves in Fluids, Elastic Waves in Solids, Electromagnetic Waves*, Academic Press, London, 1995.

[5] R.E. Kleinman and P.M. van den Berg, "Iterative methods for solving integral equations", *PIERS 5, Application of Conjugate Gradient Method to Electromagnetics and Signal Analysis*, T.K. Sarkar (Ed.), Elsevier, New York, pp. 67–102, 1991.

[6] T.D. Mast, "Empirical relationships between acoustic parameters in human soft tissues", *Acoustics Research Letters Online* vol. 1, no. 2, pp. 37–42, October 2000, and references herein.

[7] N.R. Miller, J.C. Bamber, G.R. ter Haar, "Imaging of temperature-induced echo strain: preliminary in vitro study to assess feasibility for guiding focused ultrasound surgery", *Ultrasound in Medicine and Biology*, vol. 30, no. 3, pp. 345–356, March 2004.

[8] R. Souchon, G. Bouchoux, E. Maciejko, C. Lafon, D. Cathignol, M. Bertrand and J.Y Chapelon, "Monitoring the formation of thermal lesions with heat-induced echo-strain imaging: a feasibility study", *Ultrasound in Medicine and Biology*, vol. 31, no. 2, pp. 251–259, February 2005.

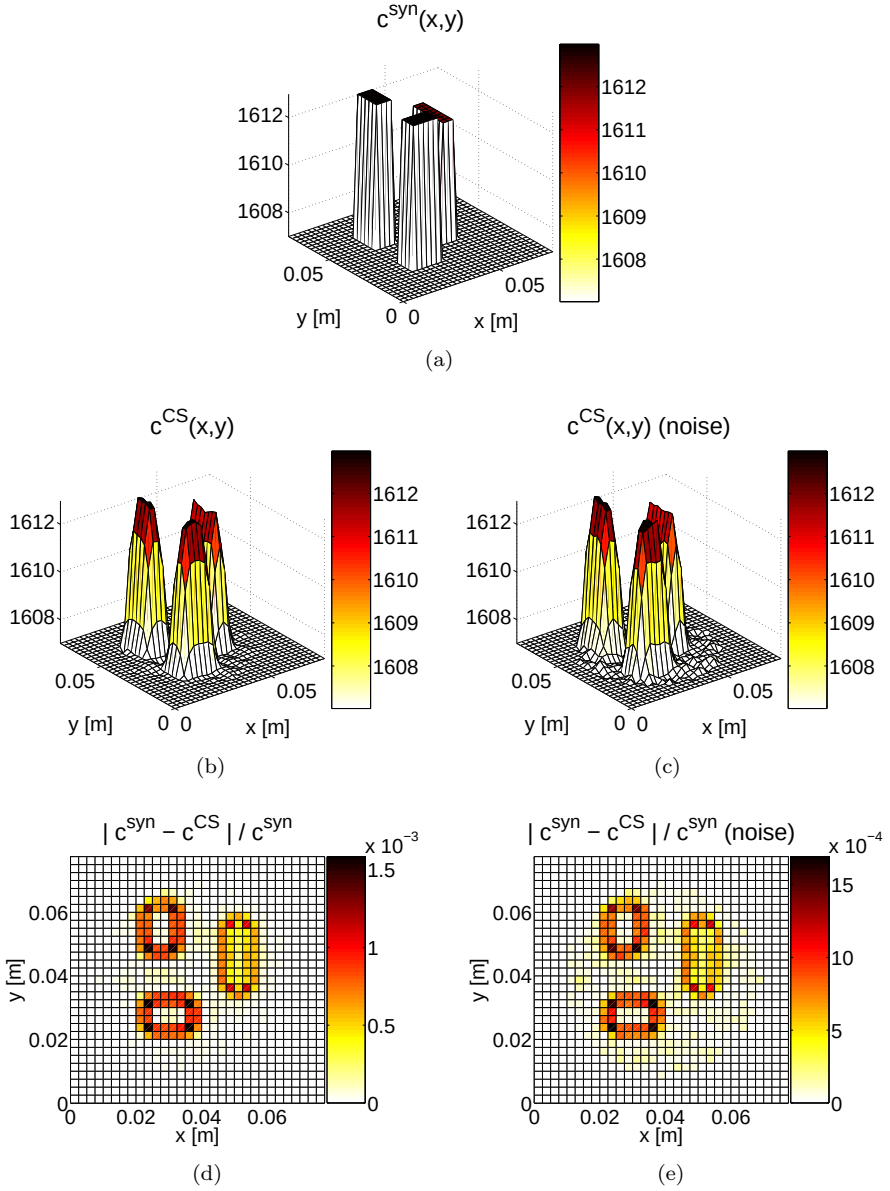

Fig. 3: A cross section of the synthetic and reconstructed velocity profiles and their relative errors.

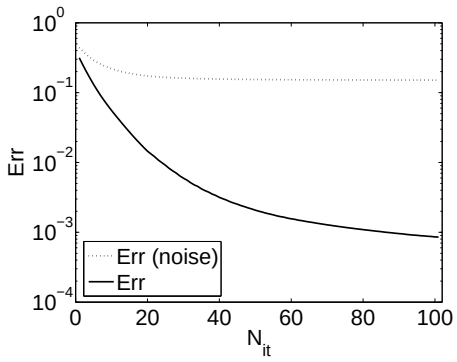

Fig. 4: The error functional Err.